JACS
JOURNAL OF THE AMERICAN CHEMICAL SOCIETY

Communication

Highly Reactive Manganese(IV)-Oxo Porphyrins Showing Temperature-Dependent Reversed Electronic Effect in C-H Bond Activation Reactions

Mian Guo, Mi Sook Seo, Yong-Min Lee, Shunichi Fukuzumi, and Wonwoo Nam

J. Am. Chem. Soc., **Just Accepted Manuscript** • DOI: 10.1021/jacs.9b04496 • Publication Date (Web): 23 Jul 2019

Just Accepted

is published by the American Chemical Society. 1155 Sixteenth Street N.W., Washington, DC 20036

Highly Reactive Manganese(IV)-Oxo Porphyrins Showing Temperature-Dependent Reversed Electronic Effect in C-H Bond Activation Reactions

Mian Guo,[†] Mi Sook Seo,[†] Yong-Min Lee,[†] Shunichi Fukuzumi,*[,†,‡] and Wonwoo Nam*[,†,§]

[†]Department of Chemistry and Nano Science, Ewha Womans University, Seoul 03760, Korea
[‡]Faculty of Science and Engineering, Meijo University, Nagoya, Aichi 468-0073, Japan
[§]School of Chemistry and Chemical Engineering, Shaanxi Normal University, Xi'an 710119, China

ABSTRACT: We report that Mn(IV)-oxo porphyrin complexes, Mn^{IV}(O)(TMP) (**1**) and Mn^{IV}(O)(TDCPP) (**2**), are capable of activating the C-H bonds of hydrocarbons, including unactivated alkanes such as cyclohexane, via an oxygen non-rebound mechanism. Interestingly, **1** with an electron-rich porphyrin is more reactive than **2** with an electron-deficient porphyrin at a high temperature (e.g., 273 K). However, at a low temperature (e.g., 233 K), the reactivity of **1** and **2** is reversed, showing that **2** is more reactive than **1**. To the best of our knowledge, the present study reports the first example of highly reactive Mn(IV)-oxo porphyrins and their temperature-dependent reactivity in C-H bond activation reactions.

High-valent metal-oxo porphyrins have been implicated as the key intermediates in the catalytic oxidation of organic substrates by heme enzymes and metalloporphyrins.[1] One example is the iron(IV)-oxo porphyrin π-cation radical species, referred to as compound I (Cpd I), in cytochromes P450.[2] In biomimetic studies, a number of iron(IV)-oxo porphyrin π-cation radicals and their one-electron reduced iron(IV)-oxo porphyrins, referred to as compound II (Cpd II), have been synthesized and investigated in various oxidation reactions.[3,4] While the high reactivity of Cpd I models has been well established in oxidation reactions, including a hydrogen atom (H-atom) abstraction of hydrocarbon C-H bonds, Cpd II models were shown to be sluggish oxidants.[3,4] In addition, the reactivity of Cpd I was shown to be affected significantly by the electronic nature of iron porphyrins; Cpd I with an electron-deficient porphyrin is much more reactive than that with an electron-rich porphyrin.[5]

Manganese porphyrins have also been used as catalysts in oxidation reactions.[3b,6] Following the heme paradigm, Mn(V)-oxo porphyrins have been proposed as the active oxidants responsible for the oxidation reactions.[1a,1c,6] However, different from the Cpd I models, Mn(V)-oxo porphyrins have been less clearly explored in characterization and reactivity studies.[7] Similarly, the reactivity of Mn(IV)-oxo porphyrins has been rarely investigated due to their low reactivity.[8] In contrast to the Mn(IV)-oxo porphyrins, however, Mn(IV)-oxo complexes with non-porphyrinic ligands have shown high reactivities in oxidation reactions.[9]

Herein, we report for the first time highly reactive Mn(IV)-oxo porphyrins in the C-H bond activation of hydrocarbons, including unactivated alkanes such as cyclohexane (Scheme 1).

Scheme 1. Structures of Mn(IV)-Oxo Porphyrins, Mn^{IV}(O)(TMP) (1) and Mn^{IV}(O)(TDCPP) (2), and Their Reaction with Cyclohexane in CH_2X_2

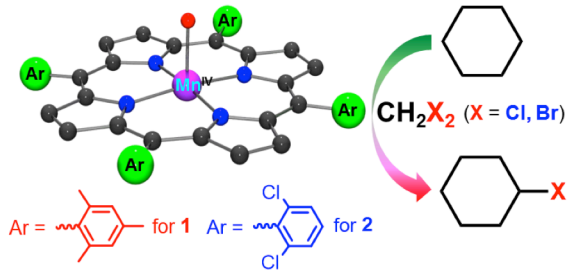

More interestingly, the Mn(IV)-oxo porphyrins show an unusual reactivity dependence on the nature of the porphyrin ligands and the reaction temperature; that is, a Mn(IV)-oxo complex bearing an electron-rich porphyrin, [Mn^{IV}(O)(TMP)] (**1**),[10] is more reactive than a Mn(IV)-oxo complex bearing an electron-deficient porphyrin, [Mn^{IV}(O)(TDCPP)] (**2**),[10] at a high temperature, whereas **2** becomes more reactive than **1** at a low temperature. Such a reversed reactivity of the Mn(IV)-oxo porphyrins depending on reaction temperatures is of significant interest in oxidation reactions by high-valent metal-oxo intermediates. Other mechanistic aspects, such as the oxygen non-rebound mechanism in Mn(IV)-oxo porphyrin system (Scheme 1), are discussed as well.

The reaction of [Mn^{III}(TMP)Cl] with 5 equiv of 1-(*tert*-butylsulfonyl)-2-iodosylbenzene (^{s}PhIO) in CH_2Cl_2 or acetone at −10 °C resulted in the change of the Soret band from 478 nm to 415 nm with clean isosbestic points (Figure 1a). The metastable intermediate ($t_{1/2}$ ~30 min at −10 °C), denoted as **1**, was characterized using various spectroscopic techniques: CSI-MS[10] spectrum of **1** exhibited a prominent ion peak at a mass-to-charge ratio (m/z) of 851.4, corresponding to [Mn(O)(TMP)] (calcd m/z = 851.4), which shifted to m/z of 853.4 (i.e., [Mn(^{18}O)(TMP)]) upon ^{18}O-substitution (Figure 1a, inset). The X-band EPR[10] spectrum of **1** showed signals at g_{eff} = 4.3, 3.7, and 2.0, suggesting a high-spin S = 3/2 Mn^{IV} species (Supporting Information, Figures S1a and S1b).[8,9] The rRaman[10] spectrum of **1** displayed one isotopically sensitive band at 803 cm^{-1}, which shifted to 767 cm^{-1} upon ^{18}O-substitution (Figure 1b). The observed isotopic shift of −36 cm^{-1} is in good agreement with the calculated value (−36 cm^{-1}) for a diatomic Mn-O

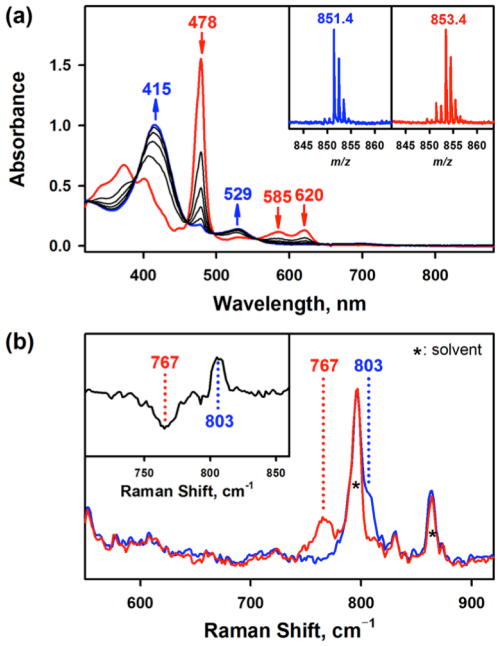

Figure 1. (a) UV-vis spectral changes showing the formation of **1** (blue line) in the reaction of [Mn^{III}(TMP)Cl] (0.10 mM, red line) and ^{s}PhIO (0.50 mM) in CH_2Cl_2 at −10 °C. Insets show the CSI-MS spectra of **1**-^{16}O (left panel) and **1**-^{18}O (right panel). (b) rRaman spectra of **1**-^{16}O (blue line) and **1**-^{18}O (red line). Inset shows the difference spectrum of **1**-^{16}O and **1**-^{18}O.

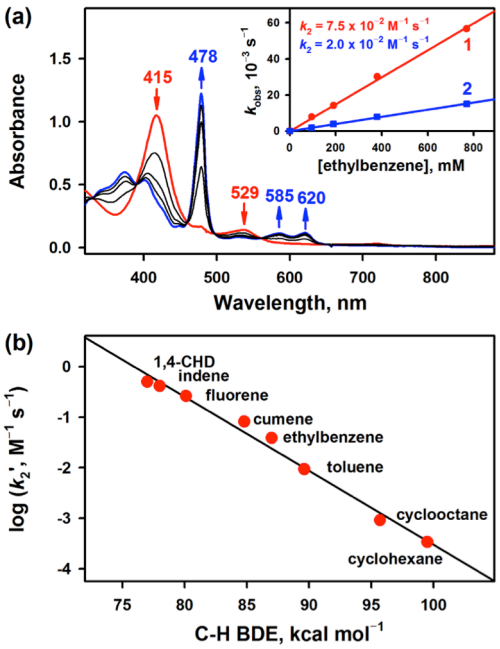

Figure 2. (a) UV-Vis spectral changes showing the reaction of **1** (0.10 mM, red line) and ethylbenzene (0.35 M) in CH_2Cl_2 at −10 °C. Inset shows the plots of k_{obs} against ethylbenzene concentration to determine k_2 values of **1** (red circles) and **2** (blue squares). (b) Plot of log k_2' (k_2' = k_2/number of equivalent target C-H bonds) against the substrate C-H BDEs.

bond oscillator. Further, the rRaman data suggest double bond character for the Mn-O bond.[8a,11]

Similarly, addition of 5 equiv of ^{s}PhIO to a solution of [Mn^{III}(TDCPP)Cl] in CH_2Cl_2 or acetone at −10 °C afforded a new intermediate ($t_{1/2}$ ~150 min at −10 °C), denoted as **2**. **2** was characterized with UV-vis, CSI-MS, EPR, and rRaman (Figures S1 – S4). Based on the results of the spectroscopic characterization, we were able to assign **1** and **2** as [Mn^{IV}(O)(TMP)] and [Mn^{IV}(O)(TDCPP)], respectively.[12]

We then investigated the reactivities of **1** and **2** in the C-H activation of hydrocarbons. Addition of ethylbenzene to a CH_2Cl_2 solution containing **1** (Figure 2a) or **2** (Figure S5b) at −10 °C afforded clean spectral changes with isosbestic points. The first-order rate constants, determined by pseudo-first-order fitting for the decay of **1** and **2** (Figure S5), increased linearly with increasing ethylbenzene concentration, giving second-order rate constants of 7.5×10^{-2} M^{-1} s^{-1} for **1** and 2.0×10^{-2} M^{-1} s^{-1} for **2** at −10 °C (Figure 2a, inset). It is of interest to note that **1** bearing an electron-rich porphyrin is more reactive than **2** bearing an electron-deficient porphyrin (vide infra). KIE[10] values of 11 and 12 were obtained in the oxidation of ethylbenzene by **1** and **2**, respectively (Figure S6).

The C-H activation reactivity of **1** was also investigated using other substrates, such as CHD,[10] indene, fluorene, cumene, toluene, cyclooctane, and cyclohexane (Figures S7 and S8), and a good linear correlation between the BDEs[10] of the substrates and the reaction rate constants was observed (Figure 2b). It should be noted that **1** is capable of activating strong C-H bonds of unactivated alkanes such as cyclohexane (BDE = 99.3 kcal mol^{-1}). Further, by comparing the k_2 values of **1** and other Mn^{IV}(O) complexes (e.g., [Mn^{IV}(O)(Bn-TPEN)]$^{2+}$,[10] which is one of the most reactive nonheme Mn(IV)-oxo complexes),[9c] we conclude that **1** is the most reactive Mn^{IV}(O) complex reported so far in heme and nonheme Mn(IV)-oxo systems.[13] Based on the large KIE value and the linear correlation between the BDEs of substrates and the rate constants, we conclude that a H-atom abstraction from substrate C-H bonds by the Mn(IV)-oxo porphyrin species is the rate-determining step (r.d.s.) in the C-H bond activation reactions (Scheme 2).

Product analysis for the reaction of **1** and toluene in CH_2Cl_2 under an Ar atmosphere revealed that [Mn^{III}(TMP)]$^{+}$ was formed as the decay product of **1** (Figure S10). Interestingly, we also found that benzyl chloride was the major organic product (82%) with a small amount of benzaldehyde (3%) (Scheme 2). In the reaction of **1** and cyclohexane, chlorocyclohexane was formed as the sole product (41%) (Scheme 2). In order to find out the source of Cl in the chlorinated products, we carried out the reactions in CH_2Br_2 instead of CH_2Cl_2. In the reactions of **1** with toluene and cyclohexane in CH_2Br_2, we obtained brominated products, such as benzyl bromide (72%) and bromocyclohexane (34%), respectively (Scheme 2).[14] These results demonstrate unambiguously that the solvent, CH_2Cl_2, was the source of Cl in the chlorinated products, but not the axial ligand (Cl^{-}) of the starting Mn^{III}(TMP)Cl complex. Further, when the reaction of **1** and toluene was performed in CH_2Cl_2 in the air, benzaldehyde was the major product (51%) with small amounts of benzyl alcohol (10%) and benzyl chloride (4%) (Scheme 2). Based on these results, we propose that the C-H activation reaction of the Mn(IV)-oxo porphyrins occurs via an oxygen non-rebound mechanism (Scheme 2), as reported in the C-H bond activation reactions of nonheme Mn(IV)-oxo complexes.[15]

Scheme 2. Proposed Mechanism for the C-H Bond Activation Reaction by Mn^{IV}-Oxo Porphyrin

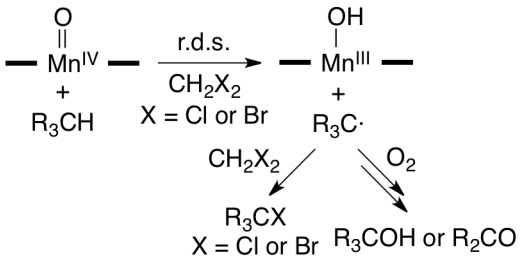

As mentioned above, the reactivity of **1** is greater than that of **2**.[16] This result is in contrary to the previously reported reactivities of iron-oxo porphyrins, in which an iron-oxo bearing an electron-deficient porphyrin (e.g., TDCPP) is a stronger oxidant than that bearing an electron-rich porphyrin (e.g., TMP).[5b] It should be noted that most of the reactivity studies with metal-oxo complexes were conducted at a lower temperature (e.g., −40 °C) due to their thermal instability.[1a,1c,5b] Since our reactivity studies were performed at a relatively high temperature (i.e., −10 °C), the reactivity of **1** and **2** was further investigated at a wide range of temperatures, such as from 0 °C to −60 °C, using CHD as a substrate. Interestingly, we found that the reactivity of **1** and **2** was reversed as the reaction temperature lowered. That is, **1** was more reactive than **2** at temperatures above −20 °C, but the reactivity was reversed and **2** became more reactive than **1** at −30 °C (Figure 3a; Table S1). Such a reversed reactivity was also observed in the reactions of indene with **1** and **2**, showing the cross point at −15 °C (Table S2 and Figure S12). This result indicates that the cross point for the reversed reactivity in the C-H activation reactions depends on the substrates. To the best of our knowledge, this is the first time to observe the reversed reactivity of high-valent metal-oxo species depending on reaction temperatures.

In order to elucidate the reversed reactivity of **1** and **2** at different temperatures, the activation enthalpies ($\Delta H^{\ddagger}$) and entropies ($\Delta S^{\ddagger}$) of **1** and **2** were determined from the Eyring plots. As shown in Figure 3a, the $\Delta H^{\ddagger}$ values in the C-H activation reactions of **1** and **2** with CHD were determined to be 10 and 6.1 kcal mol^{-1}, respectively; the lower activation enthalpy value for **2** was expected because of the higher oxidizing power of **2** bearing an electron-deficient porphyrin.[5] However, interestingly, the $\Delta S^{\ddagger}$ value of **1** was less negative than that of **2**, such as −19 vs −35 cal K^{-1} mol^{-1} for **1** and **2**, respectively (Figure 3a). Then, according to the Gibbs free energy equation (eq 1),

$$\Delta G^{\ddagger} = \Delta H^{\ddagger} - T\Delta S^{\ddagger} \quad (1)$$

the $\Delta G^{\ddagger}$ values of **1** and **2** are determined by their $\Delta S^{\ddagger}$ values depending on temperatures. For example, although the $\Delta H^{\ddagger}$ of **1** is larger than that of **2**, the $-T\Delta S^{\ddagger}$ value of **1** would be smaller than that of **2** at high temperatures. As a result, the overall $\Delta G^{\ddagger}$ of **1** is compensated and becomes smaller than that of **2** at higher temperatures (e.g., > −20 °C), illustrating the higher reactivity of **1**. In contrast, at low temperatures (e.g., < −30 °C), the $-T\Delta S^{\ddagger}$ value is not large enough to compensate the greater $\Delta H^{\ddagger}$ of **1**; therefore, $\Delta G^{\ddagger}$ of **1** becomes larger, giving a less reactivity of **1**. This phenomenon is called the "enthalpy−entropy compensation effect",[17] which is ubiquitous in various fields, such as micellization,[18] microemulsion,[19] and solution thermodynamics.[20] Moreover, it has been discussed by Fujii, van Eldik, and their co-workers that the oxidation reactions of Cpd I and Cpd II models can be controlled by the large contribution of the entropy term (i.e., $-T\Delta S^{\ddagger}$) to the free energy of activation.[21,22]

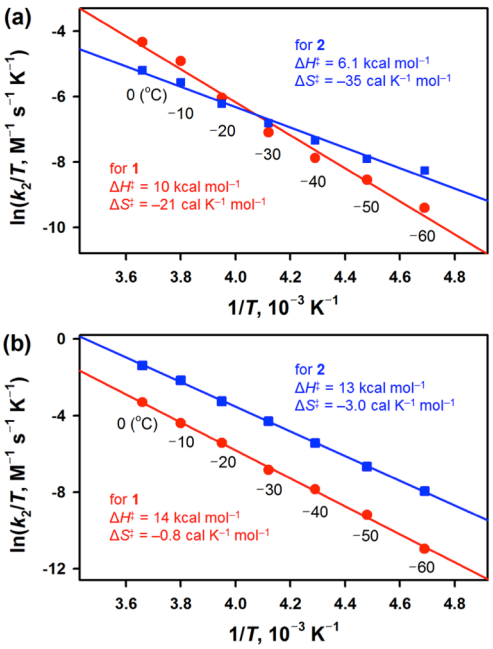

Figure 3. Eyring plots for (a) the C-H activation of CHD and (b) the electron-transfer reaction of dibromoferrocene by **1** (red circles) and **2** (blue squares).

We also investigated the electron-transfer (ET) reactions with **1** and **2**. In the ET reactions, the $\Delta S^{\ddagger}$ value is generally close to zero owing to the structureless transition state; therefore, the ET reaction is determined solely by the $\Delta H^{\ddagger}$ value.[23] Indeed, in the ET reactions of dibromoferrocene by **1** and **2**,[24] the $\Delta S^{\ddagger}$ values are close to zero (Figure 3b; Table S3). In addition, the $\Delta H^{\ddagger}$ value of **2** is smaller than that of **1** (Figure 3b). Therefore, since $\Delta G^{\ddagger}$ of **2** is always smaller than that of **1**, **2** is always more reactive than **1** irrespective of the reaction temperatures (e.g., 0 °C ~ −60 °C). This result confirms that the reversed electronic effect shown in the C-H bond activation by **1** and **2** results from the enthalpy−entropy compensation effect.

In summary, we have reported for the first time that Mn^{IV}(O) porphyrins are capable of activating the C-H bonds of hydrocarbons, affording halogenated products in halogen-containing solvents. We have also reported the first example showing the reversed reactivity of Mn^{IV}(O) porphyrins depending on reaction conditions. Our future studies will be focused on understanding the involvement of the highly reactive Mn^{IV}(O) porphyrin in catalytic oxidation reactions[6] and the enthalpy−entropy compensation effect in oxidation reactions by other metal-oxo intermediates in heme and nonheme systems.

ASSOCIATED CONTENT

Supporting Information

The Supporting Information is available free of charge via the Internet at http://pubs.acs.org.

Experimental Section, Tables S1 – S3 and Figures S1 – S12 (PDF)

AUTHOR INFORMATION

Corresponding Author

*wwnam@ewha.ac.kr
*fukuzumi@chem.eng.osaka-u.ac.jp

Notes

The authors declare no competing financial interests.

ACKNOWLEDGMENT

This work was supported by the NRF of Korea through CRI (NRF-2012R1A3A2048842 to W.N.), GRL (NRF-2010-00353 to W.N.) and Basic Science Research Program (2017R1D1A1B03029982 to Y.M.L. and 2017R1D1A1B03032615 to S.F.). W.N. acknowledges the use of resonance Raman facility at IBS (IBS-R10-A1) in Korea.

REFERENCES

(1) (a) Guo, M.; Corona, T.; Ray, K.; Nam, W. Heme and Nonheme High-Valent Iron and Manganese Oxo Cores in Biological and Abiological Oxidation Reactions. *ACS Cent. Sci.* **2019**, *5*, 13-18; (b) Dubey, K. D.; Shaik, S. Cytochrome P450—The Wonderful Nanomachine Revealed through Dynamic Simulations of the Catalytic Cycle. *Acc. Chem. Res.* **2019**, *52*, 389-399; (c) Huang, X.; Groves, J. T. Oxygen Activation and Radical Transformations in Heme Proteins and Metalloporphyrins. *Chem. Rev.* **2018**, *118*, 2491-2553; (d) Yosca, T. H.; Ledray, A. P.; Ngo, J.; Green, M. T. A New Look at the Role of Thiolate Ligation in Cytochrome P450. *J. Biol. Inorg. Chem* **2017**, *22*, 209-220; (e) Baglia, R. A.; Zaragoza, J. P. T.; Goldberg, D. P. Biomimetic Reactivity of Oxygen-Derived Manganese and Iron Porphyrinoid Complexes. *Chem. Rev.* **2017**, *117*, 13320-13352; (f) Poulos, T. L. Heme Enzyme Structure and Function. *Chem. Rev.* **2014**, *114*, 3919-3962.

(2) (a) Rittle, J.; Green, M. T. Cytochrome P450 Compound I: Capture, Characterization, and C-H Bond Activation Kinetics. *Science* **2010**, *330*, 933-937; (b) Wang, X.; Peter, S.; Kinne, M.; Hofrichter, M.; Groves, J. T. Detection and Kinetic Characterization of a Highly Reactive Heme-Thiolate Peroxygenase Compound I. *J. Am. Chem. Soc.* **2012**, *134*, 12897-12900.

(3) (a) Nam, W. High-Valent Iron(IV)–Oxo Complexes of Heme and Non-Heme Ligands in Oxygenation Reactions. *Acc. Chem. Res.* **2007**, *40*, 522-531; (b) Costas, M. Selective C–H Oxidation Catalyzed by Metalloporphyrins. *Coord. Chem. Rev.* **2011**, *255*, 2912-2932; (c) Groves, J. T.; Haushalter, R. C.; Nakamura, M.; Nemo, T. E.; Evans, B. J. High-Valent Iron-Porphyrin Complexes related to Peroxidase and Cytochrome P-450. *J. Am. Chem. Soc.* **1981**, *103*, 2884-2886.

(4) (a) Boaz, N. C.; Bell, S. R.; Groves, J. T. Ferryl Protonation in Oxoiron(IV) Porphyrins and Its Role in Oxygen Transfer. *J. Am. Chem. Soc.* **2015**, *137*, 2875-2885; (b) Jeong, Y. J.; Kang, Y.; Han, A.-R.; Lee, Y.-M.; Kotani, H.; Fukuzumi, S.; Nam, W. Hydrogen Atom Abstraction and Hydride Transfer Reactions by Iron(IV)–Oxo Porphyrins. *Angew. Chem., Int. Ed.* **2008**, *47*, 7321-7324; (c) Nam, W.; Park, S.-E.; Lim, I. K.; Lim, M. H.; Hong, J.; Kim, J. First Direct Evidence for Stereospecific Olefin Epoxidation and Alkane Hydroxylation by an Oxoiron(IV) Porphyrin Complex. *J. Am. Chem. Soc.* **2003**, *125*, 14674-14675.

(5) (a) Dolphin, D.; Traylor, T. G.; Xie, L. Y. Polyhaloporphyrins: Unusual Ligands for Metals and Metal-Catalyzed Oxidations. *Acc. Chem. Res.* **1997**, *30*, 251-259; (b) Fujii, H. Electronic Structure and Reactivity of High-Valent Oxo Iron Porphyrins. *Coord. Chem. Rev.* **2002**, *226*, 51-60.

(6) (a) Liu, W.; Groves, J. T. Manganese Catalyzed C–H Halogenation. *Acc. Chem. Res.* **2015**, *48*, 1727-1735; (b) Li, G.; Dilger, A. K.; Cheng, P. T.; Ewing, W. R.; Groves, J. T. Selective C−H Halogenation with a Highly Fluorinated Manganese Porphyrin. *Angew. Chem., Int. Ed.* **2018**, *57*, 1251-1255; (c) Liu, W.; Huang, X.; Cheng, M.-J.; Nielsen, R. J.; Goddard, W. A.; Groves, J. T. Oxidative Aliphatic C-H Fluorination with Fluoride Ion Catalyzed by a Manganese Porphyrin. *Science* **2012**, *337*, 1322-1325; (d) Collman, J.; Zhang, X.; Lee, V.; Uffelman, E.; Brauman, J. Regioselective and Enantioselective Epoxidation Catalyzed by Metalloporphyrins. *Science* **1993**, *261*, 1404-1411; (e) Battioni, P.; Renaud, J. P.; Bartoli, J. F.; Reina-Artiles, M.; Fort, M.; Mansuy, D. Monooxygenase-Like Oxidation of Hydrocarbons by Hydrogen Peroxide Catalyzed by Manganese Porphyrins and Imidazole: Selection of the Best Catalytic System and Nature of the Active Oxygen Species. *J. Am. Chem. Soc.* **1988**, *110*, 8462-8470. (f) Guo, M.; Dong, H.; Li, J.; Cheng, B.; Huang, Y.-q.; Feng, Y.-q.; Lei, A. Spectroscopic Observation of Iodosylarene Metalloporphyrin Adducts and Manganese(V)-Oxo Porphyrin Species in a Cytochrome P450 Analogue. *Nature Commun.* **2012**, *3*, 1190. (g) Hill, C. L.; Schardt, B. C. Alkane Activation and Functionalization under Mild Conditions by a Homogeneous Manganese(III)Porphyrin-Iodosylbenzene Oxidizing System. *J. Am. Chem. Soc.* **1980**, *102*, 6374-6375.

(7) (a) Song, W. J.; Seo, M. S.; DeBeer George, S.; Ohta, T.; Song, R.; Kang, M.-J.; Tosha, T.; Kitagawa, T.; Solomon, E. I.; Nam, W. Synthesis, Characterization, and Reactivities of Manganese(V)-Oxo Porphyrin Complexes. *J. Am. Chem. Soc.* **2007**, *129*, 1268-1277; (b) Jin, N.; Ibrahim, M.; Spiro, T. G.; Groves, J. T. Trans-dioxo Manganese(V) Porphyrins. *J. Am. Chem. Soc.* **2007**, *129*, 12416-12417.

(8) (a) Groves, J. T.; Stern, M. K. Synthesis, Characterization, and Reactivity of Oxomanganese(IV) Porphyrin Complexes. *J. Am. Chem. Soc.* **1988**, *110*, 8628-8638; (b) Chellaiah, A.; Yong-Min, L.; Yoon, L. J.; Shunichi, F.; Wonwoo, N. Hydrogen-Atom Abstraction Reactions by Manganese(V)– and Manganese(IV)–Oxo Porphyrin Complexes in Aqueous Solution. *Chem. - Eur. J.* **2009**, *15*, 11482-11489; (c) Fukuzumi, S.; Fujioka, N.; Kotani, H.; Ohkubo, K.; Lee, Y.-M.; Nam, W. Mechanistic Insights into Hydride-Transfer and Electron-Transfer Reactions by a Manganese(IV)−Oxo Porphyrin Complex. *J. Am. Chem. Soc.* **2009**, *131*, 17127-17134. (d) Zhang, R.; Horner, J. H.; Newcomb, M. Laser Flash Photolysis Generation and Kinetic Studies of Porphyrin−Manganese−Oxo Intermediates. Rate Constants for Oxidations Effected by Porphyrin−Mn^{V}−Oxo Species and Apparent Disproportionation Equilibrium Constants for Porphyrin−Mn^{IV}−Oxo Species. *J. Am. Chem. Soc.* **2005**, *127*, 6573-6582.

(9) (a) Parsell, T. H.; Behan, R. K.; Green, M. T.; Hendrich, M. P.; Borovik, A. S. Preparation and Properties of a Monomeric Mn^{IV}−Oxo Complex. *J. Am. Chem. Soc.* **2006**, *128*, 8728-8729; (b) Sawant, S. C.; Wu, X.; Cho, J.; Cho, K.-B.; Kim, S. H.; Seo, M. S.; Lee, Y.-M.; Kubo, M.; Ogura, T.; Shaik, S.; Nam, W. Water as an Oxygen Source: Synthesis, Characterization, and Reactivity Studies of a Mononuclear Nonheme Manganese(IV) Oxo Complex. *Angew. Chem., Int. Ed.* **2010**, *49*, 8190-8194; (c) Wu, X.; Seo, M. S.; Davis, K. M.; Lee, Y.-M.; Chen, J.; Cho, K.-B.; Pushkar, Y. N.; Nam, W. A Highly Reactive Mononuclear Non-Heme Manganese(IV)–Oxo Complex That Can Activate the Strong C–H Bonds of Alkanes. *J. Am. Chem. Soc.* **2011**, *133*, 20088-20091; (d) Leto, D. F.; Ingram, R.; Day, V. W.; Jackson, T. A. Spectroscopic Properties and Reactivity of a Mononuclear Oxomanganese(IV) Complex. *Chem. Commun.* **2013**, *49*, 5378-5380; (e) Barman, P.; Vardhaman, A. K.; Martin, B.; Wörner, S. J.; Sastri, C. V.; Comba, P. Influence of Ligand Architecture on Oxidation Reactions by High-Valent Nonheme Manganese Oxo Complexes Using Water as a Source of Oxygen. *Angew. Chem., Int. Ed.* **2015**, *54*, 2095-2099.

(10) Abbreviations used: TDCPP, *meso*-tetrakis(2,6-dichlorophenyl)porphinato dianion; TMP, *meso*-tetramesitylporphinato dianion; CSI-MS, cold spray ionization mass spectrum; EPR, electron paramagnetic resonance; rRaman, resonance Raman; KIE, kinetic isotope effect; CHD, 1,4-cyclohexadiene; BDE, bond dissociation energy; Bn-TPEN, *N*-benzyl-*N*′,*N*′,*N*′-tris(2-pyridylmethyl)-1,2-diaminoethane.

(11) (a) Terner, J.; Palaniappan, V.; Gold, A.; Weiss, R.; Fitzgerald, M. M.; Sullivan, A. M.; Hosten, C. M. Resonance Raman Spectroscopy of Oxoiron(IV) Porphyrin π-Cation Radical and Oxoiron(IV) Hemes in Peroxidase Intermediates. *J. Inorg. Biochem.* **2006**, *100*, 480-501; (b) Nakamoto, K. Resonance Raman Spectra and Biological Significance of High-Valent Iron(IV,V) Porphyrins. *Coord. Chem. Rev.* **2002**, *226*, 153-165; (c) Czernuszewicz, R. S.; Su, Y. O.; Stern, M. K.; Macor, K. A.; Kim, D.; Groves, J. T.; Spiro, T. G. Oxomanganese(IV) Porphyrins Identified by Resonance Raman and Infrared Spectroscopy. Weak Bonds and the Stability of the Half-filled t2g Subshell. *J. Am. Chem. Soc.* **1988**, *110*, 4158-4165.

(12) Lei and co-workers reported that the reaction of [Mn^{III}(TDCPP)Cl] and iodosylarene under the conditions described in this study afforded the formation of a Mn(V)(O) species without detailed spectroscopic characterization.[6f] However, the present work demonstrates unambiguously that the intermediate is not a Mn(V)(O) species but a Mn(IV)(O) species.

(13) When base was added to the solution of **1**, the UV-vis spectrum of the reaction solution indicated the formation of Mn^{IV}(O)(OH)(TMP) (Figure S9).[8a] The latter species was inactive in the C-H bond activation reactions

under the conditions (Figure S9, inset), probably due to the *trans* axial ligand effect, as shown in other $Mn^{IV}(O)(OH)$[8b] and $Mn^{V}(O)(OH)$[7a] porphyrins.

(14) 1,2-dibromoethane was detected (~20%) as a byproduct in the oxidation of toluene by **1** under Ar atmosphere in CH_2Br_2, resulting from the coupling of two $^{\bullet}CH_2Br$ radicals derived from bromine abstraction of CH_2Br_2.

(15) (a) Cho, K.-B.; Hirao, H.; Shaik, S.; Nam, W. To Rebound or Dissociate? This Is the Mechanistic Question in C-H Hydroxylation by Heme and Nonheme Metal-Oxo Complexes. *Chem. Soc. Rev.* **2016**, *45*, 1197-1210; (b) Huang, X.; Groves, J. T. Beyond ferryl-mediated hydroxylation: 40 years of the rebound mechanism and C–H activation. *J. Biol. Inorg. Chem* **2017**, *22*, 185-207.

(16) The inverted reactivity of $Mn^{IV}(O)$ porphyrins bearing electron-deficient ligands was discussed before and explained with the disproportionation of two $Mn^{IV}(O)$ to Mn^{III} and $Mn^{V}(O)$; the latter $Mn^{V}(O)$ species was then proposed as the real active oxidant in the oxidation reactions.[8d] We therefore conducted a control reaction by adding excess amount of $[Mn^{III}(TMP)Cl]$ to **1** in the reaction of ethylbenzene and found that the reaction rate was not affected (Figure S11), demonstrating that the $Mn^{IV}(O)$ porphyrin complex was the true active oxidant resposible for the C-H activation reactions in the present study.

(17) (a) Pan, A.; Biswas, T.; Rakshit, A. K.; Moulik, S. P. Enthalpy–Entropy Compensation (EEC) Effect: A Revisit. *J. Phys. Chem. B* **2015**, *119*, 15876-15884; (b) Liu, L.; Guo, Q.-X. Isokinetic Relationship, Isoequilibrium Relationship, and Enthalpy−Entropy Compensation. *Chem. Rev.* **2001**, *101*, 673-696.

(18) Chen, L.-J.; Lin, S.-Y.; Huang, C.-C. Effect of Hydrophobic Chain Length of Surfactants on Enthalpy−Entropy Compensation of Micellization. *J. Phys. Chem. B* **1998**, *102*, 4350-4356.

(19) Hait, S. K.; Moulik, S. P.; Rodgers, M. P.; Burke, S. E.; Palepu, R. Physicochemical Studies on Microemulsions. 7. Dynamics of Percolation and Energetics of Clustering in Water/AOT/Isooctane and Water/AOT/Decane w/o Microemulsions in Presence of Hydrotopes (Sodium Salicylate, α-Naphthol, β-Naphthol, Resorcinol, Catechol, Hydroquinone, Pyrogallol and Urea) and Bile Salt (Sodium Cholate). *J. Phys. Chem. B* **2001**, *105*, 7145-7154.

(20) Danil de Namor, A. F.; Sueros Velarde, F. J.; Hutcherson, R. G.; Piro, O. E.; Castellano, E. E. X-Ray Diffraction Studies and Solution Thermodynamics of 5,7,17,23-para-tert-Butyl-25,26,27,28-tetra(diethylamine)ethoxycalix(4)arene. *J. Chem. Soc., Faraday Trans.* **1998**, *94*, 1257-1261.

(21) Takahashi, A.; Kurahashi, T.; Fujii, H. Activation Parameters for Cyclohexene Oxygenation by an Oxoiron(IV) Porphyrin π-Cation Radical Complex: Entropy Control of an Allylic Hydroxylation Reaction. *Inorg. Chem.* **2007**, *46*, 6227-6229.

(22) (a) Oszajca, M.; Franke, A.; Drzewiecka-Matuszek, A.; Brindell, M.; Stochel, G.; van Eldik, R. Temperature and Pressure Effects on C–H Abstraction Reactions Involving Compound I and II Mimics in Aqueous Solution. *Inorg. Chem.* **2014**, *53*, 2848-2857; (b) Fertinger, C.; Franke, A.; van Eldik, R. Mechanistic insight from thermal activation parameters for oxygenation reactions of different substrates with biomimetic iron porphyrin models for compounds I and II. *J. Biol. Inorg. Chem* **2012**, *17*, 27-36.

(23) (a) Marcus, R. A. Electron Transfer Reactions in Chemistry: Theory and Experiment (Nobel Lecture). *Angew. Chem., Int. Ed.* **1993**, *32*, 1111-1121; (b) Fukuzumi, S. Electron-transfer properties of high-valent metal-oxo complexes. *Coord. Chem. Rev.* **2013**, *257*, 1564-1575; (c) Mader, E. A.; Manner, V. W.; Markle, T. F.; Wu, A.; Franz, J. A.; Mayer, J. M. Trends in Ground-State Entropies for Transition Metal Based Hydrogen Atom Transfer Reactions. *J. Am. Chem. Soc.* **2009**, *131*, 4335-4345; (d) Mader, E. A.; Davidson, E. R.; Mayer, J. M. Large Ground-State Entropy Changes for Hydrogen Atom Transfer Reactions of Iron Complexes. *J. Am. Chem. Soc.* **2007**, *129*, 5153-5166.

(24) The ET reactions of ferrocene by Mn^{IV}-oxo porphyrins were too fast to follow. However, reaction rate of ET of dibromoferrocene, which was of much higher oxidation pontential, was proper to obtain kinetic data. Therefore, dibromoferrocene was selected for ET study.

Table of Contents